Research Square

Preprints are preliminary reports that have not undergone peer review.
They should not be considered conclusive, used to inform clinical practice,
or referenced by the media as validated information.

Circ_0074026 Sponges miR-127-5p to Upregulate RBP7 and Promotes Hepatocellular Carcinoma Progression

Yuchen Pan
The Third Clinical Medical College of Wenzhou Medical University
Zihao Zheng
the Third Affiliated Hospital of Wenzhou Medical University
Huawei Zhai
the Third Affiliated Hospital of Wenzhou Medical University
Fujing Cai
the Third Affiliated Hospital of Wenzhou Medical University
Banglian Cai
the Third Affiliated Hospital of Wenzhou Medical University
Haifeng Zhang
the Third Affiliated Hospital of Wenzhou Medical University
Guangzheng Sun
the Third Affiliated Hospital of Wenzhou Medical University
Jinhai Li
lijindahai@126.com
the Third Affiliated Hospital of Wenzhou Medical University

Research Article

Keywords: Circ_0074026, miR-127-5p, RBP7, Hepatocellular carcinoma

Posted Date: November 13th, 2026

DOI: https://doi.org/10.21203/rs.3.rs-11323926/v1

License: This work is licensed under a Creative Commons Attribution 4.0 International License.
Read Full License

Additional Declarations: No competing interests reported.

Circ_0074026 Sponges miR-127-5p to Upregulate RBP7 and Promotes Hepatocellular Carcinoma Progression

Yuchen Pan[1†]*,Zihao Zheng*[2†]*,Huawei Zhai*[2†]*,Fujing Cai*[3]*,Banglian Cai*[4]*,Haifeng Zhang*[2*]*,Guangzheng Sun*[2*] *and Jinhai Li*[2*]

[1]*The Third Clinical Medical College of Wenzhou Medical University, Wenzhou, China.*

[2]*Department of Hepatobiliary Pancreatic Surgery, the Third Affiliated Hospital of Wenzhou Medical University, Wenzhou, Zhejiang, China.*

[3]*Department of Infectious Diseases, the Third Affiliated Hospital of Wenzhou Medical University, Wenzhou, Zhejiang, China..*

[4]*Department of Lithotripsy, the Third Affiliated Hospital of Wenzhou Medical University, Wenzhou, Zhejiang, China.*

Corresponding author: Jinhai Li, MD, Department of Hepatobiliary Pancreatic Surgery, the Third Affiliated Hospital of Wenzhou Medical University, Wenzhou, Zhejiang 325000, China(E-mail: lijindahai@126.com).Guangzheng Sun, MD, Department of Hepatobiliary Pancreatic Surgery,the Third Affiliated Hospital of Wenzhou Medical University, Wenzhou, Zhejiang 325000, China(E-mail: sunguangzheng1973@126.com).Haifeng Zhang, MD, Department of Hepatobiliary Pancreatic Surgery,the Third Affiliated Hospital of Wenzhou Medical University, Wenzhou, Zhejiang 325000, China(E-mail: zhanghaifeng197209@126.com).

Yuchen Pan, Zihao Zheng, and Huawei Zhai contributed equally to this work.

Running title: Circ_0074026/miR-127-5p/RBP7 Axis in HCC

ABSTRACT

Background: Circular RNA circ_0074026 has been identified as an oncogenic factor in glioma; however, its expression pattern, biological functions, and underlying mechanisms in hepatocellular carcinoma (HCC) remain largely unexplored. This study aimed to elucidate the regulatory mechanism of the circ_0074026/miR-127-5p/RBP7 axis in HCC progression.

Methods: The expression levels of circ_0074026, miR-127-5p, and RBP7 were measured in HCC clinical samples and cell lines by RT-qPCR. Pearson correlation analysis was performed to evaluate their interrelationships. Putative binding sites among these molecules were predicted using CircInteractome and CircBank and verified by dual-luciferase reporter and RNA pull-down assays. CCK-8 and colony formation assays were used to assess cell proliferation. Flow cytometry was performed to measure apoptosis. Scratch and Transwell assays were employed to evaluate migration and invasion. Western blotting was conducted to examine the expression of epithelial–mesenchymal transition (EMT)-related proteins.

Results: Circ_0074026 and RBP7 were significantly upregulated, whereas miR-127-5p was downregulated in HCC tissues and cells. Knockdown of circ_0074026 markedly suppressed HCC cell proliferation, migration, and invasion, promoted apoptosis, and inhibited EMT. Notably, these tumor-suppressive effects were abrogated by either miR-127-5p inhibition or RBP7 overexpression. Mechanistically, circ_0074026 directly sponged miR-127-5p, thereby relieving its repression of RBP7.

Conclusions: Our findings demonstrate that circ_0074026 drives HCC progression via the

miR-127-5p/RBP7 axis, suggesting that this circular RNA represents a potential therapeutic target for HCC patients.

Keywords： Circ_0074026; miR-127-5p; RBP7; Hepatocellular carcinoma

INTRODUCTION

Circular RNAs (circRNAs) are a class of endogenous non-coding RNAs characterized by a covalently closed loop structure, first detected in human HeLa cells[1, 2]. Recent evidence has underscored the significant roles of circRNAs in various malignancies, including HCC. For instance, circ-MTO1 inhibits HCC progression by sponging miR-9 and upregulating p21[3]; circ-TLK1 promotes HCC tumorigenesis via the miR-138-5p/SOX4 axis[4]. More recently, circ_0074026 was reported to be an unfavorable prognostic factor in glioma[5]. However, its role in HCC remains unclear.

MicroRNAs (miRNAs) are a class of small non-coding RNAs (17~25 nucleotides) that serve as useful diagnostic biomarkers and key regulators of gene expression[6]. The competing endogenous RNA (ceRNA) hypothesis has emerged as a critical mechanism in tumorigenesis, wherein circRNAs act as miRNA sponges to modulate downstream mRNA expression[7-9]. This regulatory network is intimately involved in HCC pathogenesis and holds promise for developing novel diagnostic and therapeutic strategies[10].

Despite these advances, the specific expression pattern, biological functions, and precise ceRNA regulatory network of circ_0074026 in HCC have not been fully explored. In the present study, we identified a novel circ_0074026/miR-127-5p/RBP7 axis that drives HCC progression, thereby offering a potential diagnostic biomarker and therapeutic target for this malignancy.

METHODS

Approval and ethics

The research was approved by the Ethics Committee of the Third Affiliated Hospital of Wenzhou Medical University (approval no. YJ2022006) and conducted in accordance with the Declaration of Helsinki. Written informed consent was obtained from each patient.

Clinical samples and follow-up

A total of 100 paired HCC tissues and adjacent normal tissues, preoperative serum samples from the same patients, and serum samples from 100 healthy individuals were collected. Clinicopathological features included age, sex, HBV infection, Child-Pugh grade, AFP level, tumor differentiation, tumor size, tumor multiplicity, BCLC stage, microvascular invasion (MVI), and satellite nodules. Overall survival (OS) was defined as the interval from surgery to death from any cause or the last follow-up. Progression-free survival (PFS) was defined as the interval from surgery to recurrence, progression, death, or the last follow-up. Patients were dichotomized into high- and low-expression groups using the median expression level of circ_0074026 in tissues or serum, as indicated.

Cell culture

Human HCC cell lines (SK-HEP-1 [ATCC® HTB-52™], HepG2 [ATCC® HB-8065™], Hep3B [ATCC® HB-8064™], Huh-7 [JCRB0403], and HCCLM3 [CBP60985]) and the normal liver cell line QSG-7701 [GNHu43] were obtained from the indicated repositories. All cell lines were authenticated by short tandem repeat (STR) profiling and tested negative for mycoplasma

(Beyotime, China). Cells were cultured in Dulbecco's Modified Eagle's Medium (DMEM, Gibco, USA) supplemented with 10% fetal bovine serum (FBS, Gibco) and 1% penicillin/streptomycin at 37°C in a humidified 5% CO_2 atmosphere.

Cell transfection

Small interfering RNAs (siRNAs) targeting circ_0074026 (si-circ_0074026 1# and 2#), short hairpin RNA (shRNA) targeting circ_0074026, and the pcDNA3.1 plasmid for RBP7 overexpression were supplied by AbioCenter (Jiangsu, China). Additionally, miR-127-5p mimic and inhibitor were obtained from the same source. The targeting sequences for siRNAs and shRNA are listed in Supplementary Table S1. Non-targeting siRNA (si-NC), scramble shRNA (sh-NC), empty vector (oe-NC), and negative controls for miRNA (miR-NC and anti-miR-NC) served as controls. Transfections were performed using Lipofectamine 3000 (Invitrogen, USA) according to the manufacturer's protocol.

RNA extraction and RT-qPCR

Total RNA was extracted from cells and tissues using TRIzol reagent (Invitrogen, Carlsbad, CA, USA) according to the manufacturer's instructions. Reverse transcription was performed using a PrimeScript RT Reagent Kit (TaKaRa, Dalian, China). qPCR was performed using SYBR Green Master Mix (TaKaRa) on a LightCycler 480 system (Roche, Basel, Switzerland). GAPDH was used as the internal control for circ_0074026 and RBP7, and U6 was used for miR-127-5p. Relative expression was calculated using the $2^{-\Delta\Delta Ct}$ method. For serum circRNA analysis, cel-miR-39 was used as an exogenous spike-in control. U6 stability was validated before use. Primer

sequences are listed in Table 2.

Actinomycin D and RNase R treatment assays

HCC cells were treated with actinomycin D (2 μg/mL) or RNase R (3 U/μg), as previously described[11]. Total RNA was then extracted, and the levels of circ_0074026 and linear PITX1 were measured by RT-qPCR..

Fluorescence in situ hybridization (FISH)

The circ_0074026 FISH probe was designed to target the back-splice junction sequence of circ_0074026 and was synthesized and labelled with Cy3 by RiboBio (Guangzhou, China). The probe was custom-designed based on the circ_0074026 sequence (circBase ID: hsa_circ_0074026; host gene: PITX1), with the probe sequence provided in Supplementary Table S2. A scrambled probe served as the negative control. The FISH assay was performed using the Ribo™ FISH Kit (RiboBio, Guangzhou, China) according to the manufacturer's instructions. Briefly, cells grown on coverslips were fixed in 4% paraformaldehyde for 15 min at room temperature, permeabilized with 0.5% Triton X-100 for 10 min, and pre-hybridized in hybridization buffer at 37°C for 30 min. The Cy3-labelled circ_0074026 probe was then added at a final concentration of 100 nM, and hybridization was carried out overnight at 37°C in a humidified chamber. After hybridization, the coverslips were washed sequentially with wash buffer I (2× SSC, 0.1% SDS) at 42°C for 5 min, wash buffer II (1× SSC) at 42°C for 5 min, and wash buffer III (0.1× SSC) at 42°C for 5 min. Nuclei were counterstained with DAPI (Beyotime, Shanghai, China) for 10 min at room temperature. Images were captured using a confocal laser scanning microscope (Zeiss LSM 880, Carl Zeiss, Germany) and processed with ZEN software.

Cell counting Kit-8 (CCK-8) assay

The proliferation of HCC cells was assessed using the CCK-8 assay. Transfected cells were seeded into 96-well plates and incubated at 37°C in a 5% CO_2 atmosphere. After 24, 48, or 72 hours of incubation, 10 μL of CCK-8 reagent (Transgen Biotech, Beijing, China) was added to each well. The cells were then incubated at 37°C for one hour. The optical density (OD) at 450 nm was measured using a microplate reader (Bio-Rad, USA).

Colony Formation Assay

The colony-forming ability of HCC cells was evaluated using a colony formation assay. Transfected cells were trypsinized, counted, and seeded into 6-well plates at a density of 500 cells per well. The cells were cultured at 37°C with 5% CO_2 for 12 days to allow colony formation. The medium was replaced every 3 days. When visible colonies appeared, the cells were washed with PBS, fixed with methanol for 15 minutes, and stained with 0.1% crystal violet for 20 minutes. After washing away excess stain, colonies containing more than 50 cells were counted under a microscope.

Flow cytometry

Flow cytometry was employed to examine apoptosis of HCC cells. After a 48-hour transfection, HCC cells were harvested, resuspended and double-labeled with Annexin V-FITC/PI. The apoptotic rates were analyzed by the software FlowJo (BD Biosciences, USA).

Scratch assay

A 10 μL pipette tip was used to create a scratch in the cell monolayer. Wound healing was observed at 0 and 24 h along the scratch line.

Transwell assays

Cell migration was assessed using Transwell chambers without Matrigel. For invasion assays, Transwell chambers were precoated with Matrigel (BD Biosciences, Franklin Lakes, NJ, USA). Transfected cells were resuspended in serum-free DMEM and added to the upper chamber. The lower chamber was filled with DMEM containing 10% FBS. After 24 h, cells that had migrated or invaded to the lower surface were fixed with methanol and stained with crystal violet.

Luciferase reporter assay

Circ_0074026-wt (wild-type), RBP7-wt, and their mutants (circ_0074026-mut and RBP7-mut) were constructed and purchased from AbioCenter (Jiangsu, China). These reporters were then co-transfected with miR-127-5p mimics or NC mimics intoHep3B and HCCLM3 cells. Luciferase activity was then measured using the Dual-Luciferase Reporter Assay System (Promega, USA)

according to the manufacturer's instructions.

Western blot

Total proteins were extracted using RIPA lysis buffer (Beyotime, Shanghai, China) supplemented with protease and phosphatase inhibitors. Protein concentration was determined using a BCA Protein Assay Kit (Beyotime, Shanghai, China). Equal amounts of protein (30 μg) were separated by 10% SDS-PAGE and transferred onto nitrocellulose membranes (Millipore, Billerica, MA, USA). The membranes were blocked with 5% non-fat dry milk in TBST for 1 h at room temperature and then incubated overnight at 4°C with the following primary antibodies: anti-E-cadherin (Proteintech, Wuhan, China; Cat. No. 20874-1-AP; 1:2,000), anti-N-cadherin (Proteintech, Wuhan, China; Cat. No. 22018-1-AP; 1:1,000), anti-vimentin (Proteintech, Wuhan, China; Cat. No. 10366-1-AP; 1:5,000), and anti-GAPDH (Proteintech, Wuhan, China; Cat. No. 60004-1-Ig; 1:50,000). After washing with TBST, the membranes were incubated with HRP-conjugated goat anti-rabbit (Proteintech, Wuhan, China; Cat. No. SA00001-2; 1:5,000) or goat anti-mouse (Proteintech, Wuhan, China; Cat. No. SA00001-1; 1:5,000) secondary antibodies for 1 h at room temperature. Protein bands were visualized using an enhanced chemiluminescence (ECL) system (Thermo Fisher Scientific, Waltham, MA, USA) and quantified with ImageJ software (National Institutes of Health, Bethesda, MD, USA). GAPDH was used as the loading control. All experiments were performed in triplicate.

RNA pull-down assay

Biotin-labeled miR-127-5p or negative control was incubated with cell lysates. The RNA–protein complexes were pulled down with streptavidin beads. The enrichment of circ_0074026 and RBP7 mRNA was assessed by RT-qPCR. Non-specific binding was controlled using a biotin-labeled scramble probe.

Animal models

Mice were randomly assigned to groups. Investigators measuring tumor volume and metastatic nodules were blinded to group allocation. Stable knockdown of circ_0074026 was confirmed by RT-qPCR before inoculation.The research was approved by the Animal Ethics

Committee of Wenzhou Medical University (approval no. XMSQ-2024-025). Four-week-old female BALB/c nude mice weighing 10-15 grams were procured from Gempharmatech (Nanjing, China). For the subcutaneous tumorigenesis model, Hep3B cells (1×10^6 in 100 μL PBS) stably transfected with sh-NC or sh-circ_0074026 were implanted subcutaneously into the right armpit of each mouse (n = 6 per group). Tumor dimensions were measured twice weekly with calipers, and tumor volumes (V) were calculated using the formula $V = ½ \times a \times b^2$, where "a" and "b" denoted the larger and smaller tumor axes (in millimeters). Mice were euthanized 28 days post-inoculation, and tumors were excised, weighed, and photographed. For the experimental metastasis model, Hep3B cells (1.5×10^6 in 100 μL PBS) transfected with sh-NC or sh-circ_0074026 were administered intravenously via the tail vein (n = 5 per group). After 6 weeks, the mice were euthanized; lungs were harvested, fixed in Bouin's solution, and metastatic nodules on the lung surface were counted under a dissecting microscope. All animal procedures were performed in accordance with the ARRIVE guidelines and the National Institutes of Health Guide for the Care and Use of Laboratory Animals.

Immunohistochemistry (IHC)

Ki-67 expression in xenograft tumour tissues was examined by IHC. Briefly, paraffin-embedded sections (4 μm) were deparaffinized in xylene and rehydrated through a graded ethanol series. Antigen retrieval was performed by heating the sections in 10 mmol/L citrate buffer (pH 6.0) in a microwave oven for 15 min. After cooling to room temperature, endogenous peroxidase activity was blocked with 3% H_2O_2 for 10 min, followed by blocking with 5% bovine serum albumin (BSA) for 30 min at room temperature. Sections were then incubated with an anti-Ki-67 primary antibody (Servicebio, Wuhan, China; Cat. No. GB111499; 1:500 dilution) overnight at 4°C. After washing with PBS, sections were incubated with an HRP-conjugated secondary antibody (Servicebio, Wuhan, China; Cat. No. GB23303; 1:200 dilution) for 50 min at room temperature. Immunoreactivity was visualized using a DAB chromogen kit (Servicebio, Wuhan, China; Cat. No. G1212) according to the manufacturer's instructions, and sections were counterstained with haematoxylin. Cells showing uniform Ki-67 staining were considered positive.

The percentage of Ki-67-positive cells was calculated by counting at least three randomly selected high-power fields (400×) per sample using ImageJ software (National Institutes of Health, Bethesda, MD, USA).

Bioinformatics analysis

The potential miRNAs targeting circ_0074026 were predicted using CircInteractome (https://circinteractome.nia.nih.gov/) and CircBank (http://www.circbank.cn/). The putative downstream mRNAs of miR-127-5p were predicted using TargetScan (https://www.targetscan.org/), miRDB (http://mirdb.org/), and ENCORI (https://rnasysu.com/encori/). Genes predicted by at least two databases were considered candidate targets. The predicted binding sites were visualized using the corresponding database output.

Diagnostic and prognostic analyses

Receiver operating characteristic (ROC) curve analysis was performed to evaluate the diagnostic value of serum circ_0074026 for distinguishing HCC patients from healthy controls, and the area under the curve (AUC) with 95% confidence interval (*CI*) was calculated. Kaplan-Meier analysis with the log-rank test was used to compare OS and PFS between high- and low-expression groups. Univariate logistic regression was used to assess the association between serum circ_0074026 expression and clinicopathological characteristics (Table 3). Variables with $P < 0.05$ in univariate analysis were included in multivariate Cox proportional hazards regression to identify independent prognostic factors for OS (Table 4). A nomogram was constructed based on clinicopathological variables and circ_0074026 to predict 1-, 3-, and 5-year OS probabilities. Calibration curves were generated to assess the agreement between nomogram-predicted and observed OS. $P < 0.05$ was considered statistically significant.

Statistical analysis

All data are expressed as mean ± standard deviation (SD). Student's t-test or one-way ANOVA was used for comparisons between groups using *SPSS* 22.0 (IBM, Chicago, IL, USA). Overall

survival was assessed using the Kaplan–Meier method. Correlations between miR-127-5p and circ_0074026 or RBP7 were analyzed using Pearson correlation analysis. Univariate Cox proportional hazards regression was used to identify factors associated with overall survival. Variables with $P < 0.05$ in univariate analysis were included in multivariate Cox regression analysis. Univariate logistic regression was used separately to assess factors associated with high serum circ_0074026 expression (Table 3). Statistical significance was defined as $P < 0.05$.

RESULTS

Identification and expression of circ_0074026 in HCC

Bioinformatics analysis of differentially expressed circRNAs was conducted using high-throughput RNA-seq of three paired HCC clinical samples and adjacent tissues (Fig. 1A). A total of 544 differentially expressed circRNAs were identified from GSE155367, of which 386 were upregulated and 158 were downregulated (Fig. 1B). To identify candidate circRNAs for further validation, we intersected differentially expressed circRNAs with KEGG pathway-related circRNAs. The Venn diagram showed 668 circRNAs in one set and 256 circRNAs in the other set, with 7 candidate circRNAs (Fig. 1C). These 7 candidate circRNAs were then subjected to RT-qPCR validation in QSG-7701, Hep3B, and HCCLM3 cells (Fig. 1D). Meanwhile, RT-qPCR revealed that circ_0074026 expression was significantly higher in HCC cell lines (SK, HepG2, Hep3B, Huh-7, and HCCLM3) than in the normal hepatocyte cell line (QSG-7701), with the highest expression observed in Hep3B and HCCLM3 (Fig. 1E). Therefore, Hep3B and HCCLM3 were selected for subsequent experiments. The stability of circ_0074026 was demonstrated by actinomycin D and RNase R treatments. The results showed that the expression of linear PITX1 decreased following actinomycin D or RNase R treatment. Owing to its circular structure, circ_0074026 was resistant to both actinomycin D and RNase R treatment (Fig. 1F-G). RNA fluorescence in situ hybridization (FISH) revealed that circ_0074026 was predominantly localized in the cytoplasm, suggesting its involvement in the regulation of HCC progression (Fig. 1H). Collectively, these results demonstrate that circ_0074026, which is mainly localized in the

cytoplasm, possesses a stable circular structure and is upregulated in HCC tissues and cells.

Circ_0074026 was upregulated in HCC and predicted a poor prognosis

We next examined circ_0074026 expression in HCC clinical samples. Circ_0074026 was significantly upregulated in HCC tissues compared with paired adjacent normal tissues (Fig. 2A) and in unpaired tumor tissues compared with normal tissues (Fig. 2B). Higher circ_0074026 expression was associated with larger tumor size (≥5 cm), advanced T stage (T3/T4), BCLC stage C, presence of MVI, higher AFP level (≥400 ng/mL), and poorer tumor differentiation (Fig. 2C–I). Serum circ_0074026 yielded an AUC of 0.913 (95% *CI* 0.623~0.976, $P < 0.001$) for discriminating HCC patients from healthy controls (Fig. 2J). Survival analysis showed that patients with high circ_0074026 expression had significantly shorter OS (HR = 2.63, 95% *CI* 1.83~3.68, $P < 0.001$; Fig. 2K) and PFS (HR = 1.85, 95% *CI* 1.36~2.52, $P = 0.001$; Fig. 2L) than those with low expression. Univariate logistic regression revealed that high serum circ_0074026 expression was significantly associated with AFP level (OR =1.287, $P = 0.0011$), tumor differentiation (OR = 4.489, $P = 0.0021$), tumor size (OR = 3.389, $P = 0.0142$), BCLC stage (OR = 3.472, $P = 0.0338$), MVI (OR = 1.637, $P = 0.0112$), and satellite nodules (OR = 2.898, $P = 0.0353$) (Table 3). Multivariate Cox regression analysis further identified high serum circ_0074026 expression as an independent unfavorable prognostic factor for OS (HR = 3.479, 95% *CI* 1.865~6.491, $P = 0.001$), together with poor tumor differentiation (HR = 2.449, 95% *CI* 1.253~4.786, $P = 0.009$) and tumor size ≥5cm (HR = 2.063, 95% *CI* 1.001~4.253, $P = 0.050$) (Table 4). A nomogram incorporating clinicopathological variables and circ_0074026 was constructed to predict 1-, 3-, and 5-year OS probabilities (Fig. 2M), and calibration curves showed good agreement between predicted and observed survival (Fig. 2N). These findings indicate that circ_0074026 is upregulated in HCC and may serve as a diagnostic and prognostic biomarker.

=

Knockdown of circ_0074026 inhibited the malignant progression of HCC cells

To investigate the role of circ_0074026 in HCC cells, two siRNA sequences (si-circ_0074026 1# and 2#) were designed. RT-qPCR revealed that both siRNAs significantly downregulated circ_0074026 expression in Hep3B and HCCLM3 cells. Notably, si-circ_0074026 1# showed a better knockdown effect (Fig. 3A). CCK-8 assays demonstrated that circ_0074026 knockdown significantly suppressed the proliferation of HCC cells (Fig. 3B), and colony formation assays showed that circ_0074026 knockdown markedly decreased the number of colonies formed by HCC cells (Fig. 3C). Flow cytometry showed an increased apoptotic rate after circ_0074026 knockdown (Fig. 3D). Scratch and Transwell assays showed that circ_0074026 knockdown inhibited the migration and invasion of HCC cells (Fig. 3E-G). Previous research has suggested that EMT significantly influences the malignancy of HCC[12, 13]. Recent studies have indicated that circRNAs play a vital role in regulating EMT in HCC cells[14-16]. RT-qPCR and western blot revealed that circ_0074026 knockdown led to a notable increase in E-cadherin expression and a significant reduction in N-cadherin and vimentin expression (Fig. 3H-K). Collectively, these data confirm that circ_0074026 promotes HCC cell proliferation, migration, invasion, and EMT, while inhibiting apoptosis.

Circ_0074026 functions as a molecular sponge for miR-127-5p in HCC

Given that circ_0074026 was predominantly localized in the cytoplasm, we next investigated whether it could function as a competing endogenous RNA (ceRNA) by sponging miRNAs. Bioinformatics analysis using CircInteractome and CircBank predicted miR-127-5p as a potential

downstream miRNA of circ_0074026 (Fig. 4A). Dual-luciferase reporter assays showed that miR-127-5p mimics markedly decreased the luciferase activity of the circ_0074026 wild-type (wt) reporter, whereas the mutant (mut) reporter was unaffected (Fig. 4B). Consistent with this, RNA pull-down assays demonstrated that biotin-labeled miR-127-5p significantly enriched circ_0074026 compared with the negative control (Fig. 4C). RT-qPCR analysis further revealed that miR-127-5p was significantly downregulated in HCC cell lines (Hep3B and HCCLM3) relative to the normal hepatocyte line QSG-7701 (Fig. 4D), as well as in HCC tissues compared with adjacent normal tissues (Fig. 4E). Pearson correlation analysis showed a significant inverse correlation between circ_0074026 and miR-127-5p expression in HCC tissues ($R = -0.2321$, $P < 0.001$; Fig. 4F). Moreover, knockdown of circ_0074026 significantly increased miR-127-5p expression in Hep3B and HCCLM3 cells (Fig. 4G). Collectively, these findings indicate that circ_0074026 directly interacts with miR-127-5p and functions as a molecular sponge for miR-127-5p in HCC.

Inhibition of miR-127-5p reversed the impacts of circ_0074026 knockdown on HCC progression

RT-qPCR was employed to evaluate the effect of the miR-127-5p inhibitor. The results demonstrated that miR-127-5p expression was notably suppressed in HCC cells following transfection with the miR-127-5p inhibitor (Fig. 5A). Knockdown of circ_0074026 expression significantly inhibited proliferation, migration, invasion, and EMT, while promoting apoptosis in HCC cells. These effects were reversed by the miR-127-5p inhibitor (Fig. 5B-K).

Circ_0074026 sponged miR-127-5p and positively modulated RBP7 expression

TargetScan, miRDB, and ENCORI predicted RBP7 as a putative downstream target of miR-127-5p, with a complementary binding site in the RBP7 3′-untranslated region (Fig. 6A). Dual-luciferase reporter assays in Hep3B and HCCLM3 cells demonstrated that miR-127-5p mimics significantly reduced the luciferase activity of the RBP7 wild-type (wt) reporter, whereas the mutant (mut) reporter was unaffected (Fig. 6B). In parallel, RNA pull-down assays showed that biotin-labeled miR-127-5p significantly enriched RBP7 compared with the negative control (Fig. 6C). RT-qPCR analysis further revealed that RBP7 was markedly upregulated in HCC cell lines (Hep3B and HCCLM3) relative to the normal hepatocyte line QSG-7701 (Fig. 6D), as well as in HCC tissues compared with adjacent normal tissues (Fig. 6E). Pearson correlation analysis showed that RBP7 expression was inversely correlated with miR-127-5p expression ($R = 0.1932$, $P < 0.001$; Fig. 6F) and positively correlated with circ_0074026 expression ($R = 0.8147$, $P < 0.001$; Fig. 6G) in HCC tissues. Moreover, knockdown of circ_0074026 decreased RBP7 expression, and this reduction was reversed by co-transfection with a miR-127-5p inhibitor (Fig. 6H). Collectively, these findings indicate that circ_0074026 functions as a molecular sponge for miR-127-5p and positively modulates RBP7 expression in HCC.

Upregulation of RBP7 reversed the impacts of enhancing miR-127-5p expression on HCC progression

To investigate whether miR-127-5p participates in HCC cell progression through RBP7, several experiments were conducted. First, RBP7 expression was significantly induced by

transfection with the RBP7/pcDNA3.1 plasmid (Fig. 7A). Enhanced expression of miR-127-5p was found to inhibit HCC cell proliferation, migration, invasion, and EMT, while promoting apoptosis. Moreover, these effects could be reversed by RBP7 overexpression (Fig. 7B-K).

Circ_0074026 promoted the growth and metastasis of HCC in vivo.

An in vivo xenograft experiment demonstrated that knockdown of circ_0074026 significantly inhibited the growth of HCC cells (Fig. 8A-C). Ki-67 staining of the xenograft tumors revealed a reduced percentage of Ki-67-positive cells in the sh-circ_0074026 group compared to the sh-NC group (Fig. 8D-E). Furthermore, knockdown of circ_0074026 expression in HCC cells led to a reduced incidence of lung metastasis (Fig. 8F-H).

DISCUSSION

Circular RNAs (circRNAs) are a class of covalently closed non-coding RNAs generated by back-splicing of exons or introns[17, 18]. They participate in numerous cancer-related processes, including cell proliferation, differentiation, apoptosis, and metastasis[16,19-21].Increasing evidence has demonstrated that circRNAs play regulatory roles in HCC progression. For example, circ_0001955 promotes HCC cell progression both in vitro and in vivo by sponging miR-516a-5p and upregulating the downstream targets TRAF6 and MAPK11[22, 23]. In the present study, a heatmap of three paired HCC clinical samples and adjacent tissues revealed differentially expressed circRNAs. Using the GEO2R tool for the GSE155367 dataset, a volcano plot was generated to visualize upregulated and downregulated circRNAs in HCC. The seven most upregulated circRNAs were screened by bioinformatics analysis and validated in HCC cell lines. Among them, circ_0074026 exhibited the highest level of upregulation. Additionally, elevated circ_0074026 levels were detected in the serum of HCC patients. In-depth analysis of the clinical information of the enrolled HCC patients revealed that higher circ_0074026 expression was associated with advanced T stage or BCLC stage, poorer differentiation, larger tumor size, lower 5-year survival rate after surgery, and higher recurrence and metastasis rates.

Beyond its oncogenic role in HCC pathogenesis, our findings reveal a compelling translational dimension: serum circ_0074026 exhibited remarkable diagnostic accuracy, with an area under the curve (AUC) of 0.913, effectively distinguishing HCC patients from healthy controls. This high discriminative power is particularly noteworthy given the inherent limitations of alpha-fetoprotein (AFP), the current gold-standard serum biomarker, which suffers from suboptimal sensitivity (approximately 60~70%) and is often elevated in non-malignant hepatic conditions [24, 25]. The intrinsic covalently closed loop structure of circRNAs confers exceptional resistance to exonuclease-mediated degradation, rendering them inherently more stable than linear mRNAs in peripheral blood. Consequently, circ_0074026 represents a promising, non-invasive, and easily quantifiable candidate for the early detection of HCC, especially for AFP-

negative patients or those with indeterminate imaging findings. However, we acknowledge that the diagnostic performance demonstrated in this study was derived from a single-center cohort. Before clinical translation, several challenges must be addressed: (I) the diagnostic cut-off value requires rigorous validation in large-scale, multicenter prospective cohorts; (II) the specificity of circ_0074026 for HCC must be evaluated against other benign hepatic pathologies, such as chronic hepatitis B and cirrhosis, which are prevalent in high-risk populations; and (III) standardized pre-analytical and qPCR protocols are essential to ensure inter-laboratory reproducibility. Nevertheless, incorporating serum circ_0074026 into current surveillance algorithms, particularly when combined with AFP and imaging modalities, could provide a cost-effective and clinically actionable strategy for the early interception of HCC, ultimately improving patient outcomes.

To elucidate the role of circ_0074026 in HCC, we investigated its influence on cell proliferation, migration, invasion, EMT, and apoptosis in Hep3B and HCCLM3 cells. Our results showed that knockdown of circ_0074026 suppressed proliferation, migration, invasion, and EMT, and promoted apoptosis. CircRNAs are characterized by remarkable stability, abundance, evolutionary conservation, and tissue-specific expression. Recent discoveries have uncovered that circRNAs can serve as competing endogenous RNAs (ceRNAs) to sponge target miRNAs and thereby modulate mRNA expression. For example, circRNA-100338 promotes hepatocarcinogenesis through competitive binding to miR-141-3p and by regulating RHEB expression.^24 By FISH, we found that circ_0074026 was predominantly localized in the cytoplasm of HCC cells, suggesting that circ_0074026 may exert its regulatory role via a ceRNA mechanism. miRNAs play a crucial role in the ceRNA regulatory system. In this study, miR-127-5p was identified as a downstream target of circ_0074026 by bioinformatics prediction. Lower expression of miR-127-5p was detected in HCC cell lines and clinical samples compared with corresponding normal controls. Pearson correlation analysis showed an inverse relationship between miR-127-5p and circ_0074026. Dual-luciferase reporter and RNA pull-down assays confirmed specific binding between circ_0074026 and miR-127-5p. A series of functional assays

and rescue experiments further verified that miR-127-5p inhibition reversed the suppressive effects of circ_0074026 knockdown on HCC cell proliferation, migration, invasion, and EMT, and inhibited HCC cell apoptosis. Therefore, circ_0074026 accelerates HCC progression by modulating miR-127-5p.

Previous research has reported that miRNAs are a class of short non-coding RNA molecules that function in RNA silencing and post-transcriptional regulation of gene expression[26, 27].Studies have revealed that RBP7, located on human chromosome 1p36.22, belongs to the retinol-binding protein family and contributes to the stability and metabolism of vitamin A[28, 29].Vitamin A and its derivatives are involved in several biological processes, including cell growth, differentiation, and apoptosis[30, 31]. Notably, RBP7 has been reported to act as a tumor suppressor in HR+ breast cancer by inhibiting the AKT/SREBP1 pathway and reducing fatty acid synthesis[32]. In contrast, RBP7 has also been linked to tumor invasion and EMT in colon cancer, where it serves as a clinically prognostic biomarker[33].These seemingly contradictory findings suggest that RBP7 may exert context-dependent functions depending on the tissue type and tumor microenvironment. In the present study, RBP7 was upregulated in HCC cells and clinical samples, and its expression was positively correlated with circ_0074026 and inversely correlated with miR-127-5p. Knockdown of circ_0074026 reduced RBP7 expression, an effect that was reversed by miR-127-5p inhibition. Moreover, RBP7 overexpression reversed the inhibitory effects of miR-127-5p mimics on HCC cell proliferation, migration, invasion, and EMT. Collectively, these findings suggest that RBP7 may act as an oncogenic factor in HCC, at least in part through the circ_0074026/miR-127-5p axis. Further studies are needed to determine the molecular basis of this tissue-specific and cancer-type-specific role of RBP7, including its downstream signaling pathways and interacting proteins in HCC.

In summary, this study identified, for the first time, the ceRNA regulatory network of the circ_0074026/miR-127-5p/RBP7 axis in HCC progression. These findings reveal the regulatory mechanism by which circ_0074026 affects HCC proliferation, migration, invasion, apoptosis,

EMT, and metastasis, and may provide a new strategy for the early diagnosis and treatment of HCC patients. Nevertheless, further multicenter studies with larger sample sizes and mechanistic investigations are warranted to validate the clinical utility of circ_0074026 as a diagnostic and therapeutic target for HCC.

CONCLUSIONS

In summary, this study identified, for the first time, the ceRNA regulatory network of the circ_0074026/miR-127-5p/RBP7 axis in HCC progression（Fig.9）. These findings reveal the regulatory mechanism by which circ_0074026 affects HCC proliferation, migration, invasion, apoptosis, EMT, and metastasis, and may provide a new strategy for the early diagnosis and treatment of HCC patients.

Ethics approval and consent to participate: All aspects of this study were approved by the Research Ethics Committee of the Third Affiliated Hospital of Wenzhou Medical University.

Consent for publication: Informed consent was obtained from all subjects involved in the study.

Data Availability Statement: The datasets generated in the current study are available from the corresponding authors on reasonable request.

Conflict of interest disclosure: The authors have no relevant financial or non-financial interests to disclose.

Funding: This work was supported by Medical and Health Science Program of Zhejiang Province (Grant No. 2025HY1115), Wenzhou Municipal Science and Technology Bureau Applied Basic Research Project (Grant No. GK2025117), and Innovation Special Fund of Ruian Science and Technology Bureau (Grant No. MS2024001).

Acknowledgments: The authors thank all patients who participated in this study. We appreciate the support from the Department of Hepatobiliary Pancreatic Surgery and the Experimental Research Center at the Third Affiliated Hospital of Wenzhou Medical University.

Authors Contributions Statement : Yuchen Pan , Zihao Zheng , Huawei Zhai ,Fujing Cai and Banglian Cai wrote the draft and performed the experiments. Jinhai Li , Haifeng Zhang and Guangzheng Sun designed and supervised the study. All authors reviewed and approved the final manuscript.

REFERENCES

[1] Becker H F, Ferreira-Cerca S. Circular RNAs in Archaea[J]. Adv Exp Med Biol, 2025, 1485: 451-464.

[2] Boo S H, Shin M K, Hwang H J, et al. Circular RNAs trigger nonsense-mediated mRNA decay[J]. Mol Cell, 2024, 84(24): 4862-4877.e4867.

[3] Han D, Li J, Wang H, et al. Circular RNA circMTO1 acts as the sponge of microRNA-9 to suppress hepatocellular carcinoma progression[J]. Hepatology (Baltimore, Md), 2017, 66(4): 1151-1164.

[4] Lu Y, Liu Y, Zhang K, et al. Circular RNA TLK1 Exerts Oncogenic Functions in Hepatocellular Carcinoma by Acting as a ceRNA of miR-138-5p[J]. Journal of oncology, 2022, 2022: 2415836.

[5] Chen M, Liu X, Xie P, et al. Circular RNA circ_0074026 indicates unfavorable prognosis for patients with glioma and facilitates oncogenesis of tumor cells by targeting miR-1304 to modulate ERBB4 expression[J]. Journal of cellular physiology, 2020, 235(5): 4688-4697.

[6] Zhang Y, Zhang Q, Weng X, et al. NEase-based amplification for detection of miRNA, multiple miRNAs and circRNA[J]. Analytica chimica acta, 2021, 1145: 52-58.

[7] Nejadi Orang F, Abdoli Shadbad M. Competing endogenous RNA networks and ferroptosis in cancer: novel therapeutic targets[J]. Cell Death Dis, 2024, 15(5): 357.

[8] Zhu J, Mo Y Y, Peng W X. RNA binding protein-mediated competing endogenous RNA mechanism in cancer[J]. Gene, 2025, 963: 149606.

[9] Verma D, Siddharth S, Yende A S, et al. LUCAT1-Mediated Competing Endogenous RNA (ceRNA) Network in Triple-Negative Breast Cancer[J]. Cells, 2024, 13(22).

[10] Shi H Q, Huang S, Ma X Y, et al. BCAR3 and BCAR3-related competing endogenous RNA expression in hepatocellular carcinoma and their prognostic value[J]. World J Gastrointest Oncol, 2024, 16(7): 3082-3096.

[11] Li J, Qian L, Ge M, et al. hsa_circ_0000518 stimulates the malignant progression of hepatocellular carcinoma via regulating ITGA5 to activate the Warburg effect[J]. Cellular signalling, 2024, 120: 111243.

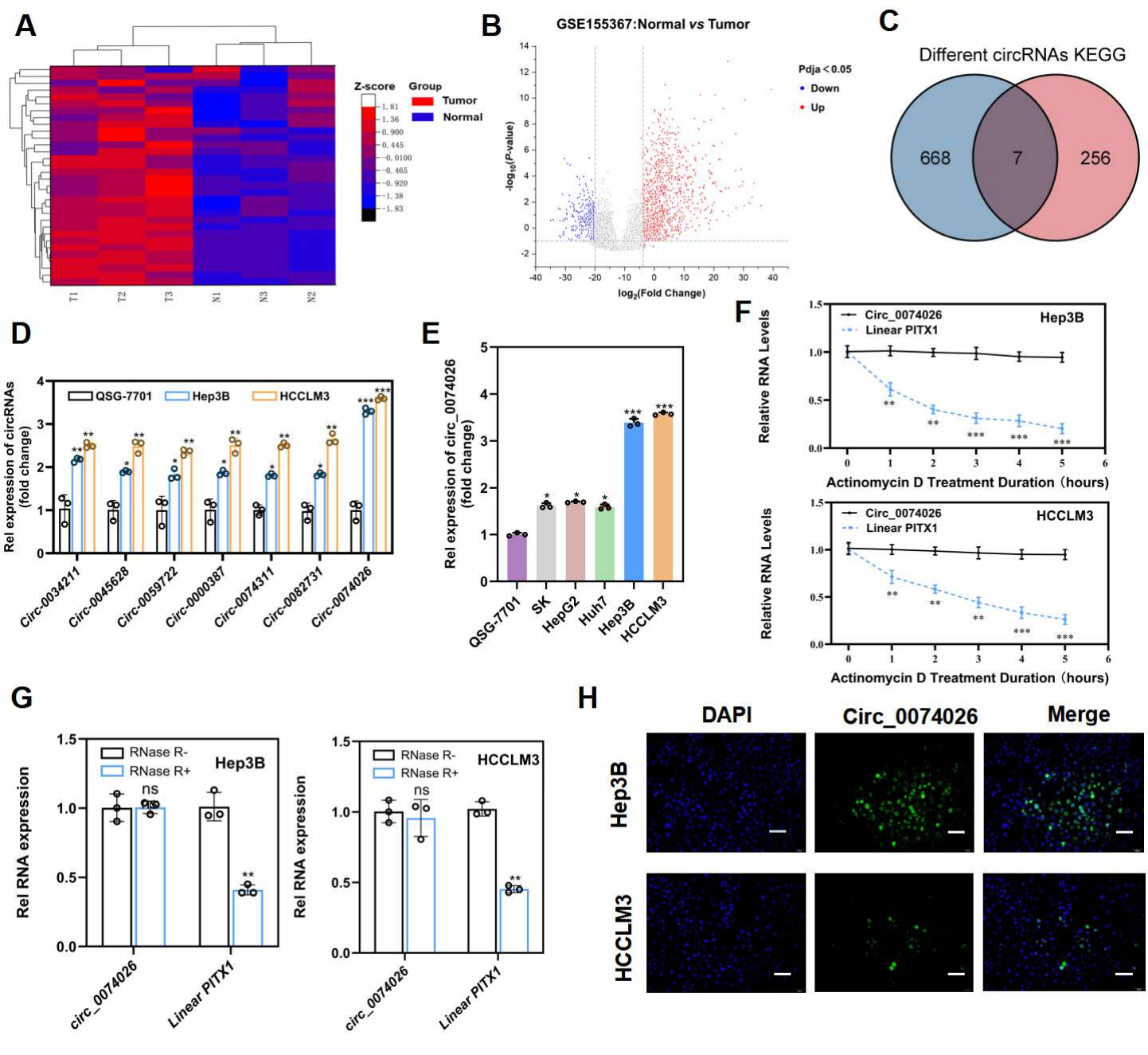
[12] Li D, Lin X, Li J, et al. Eleven metabolism-related genes composed of Stard5 predict prognosis and contribute to EMT phenotype in HCC[J]. Cancer cell international, 2023, 23(1): 277.

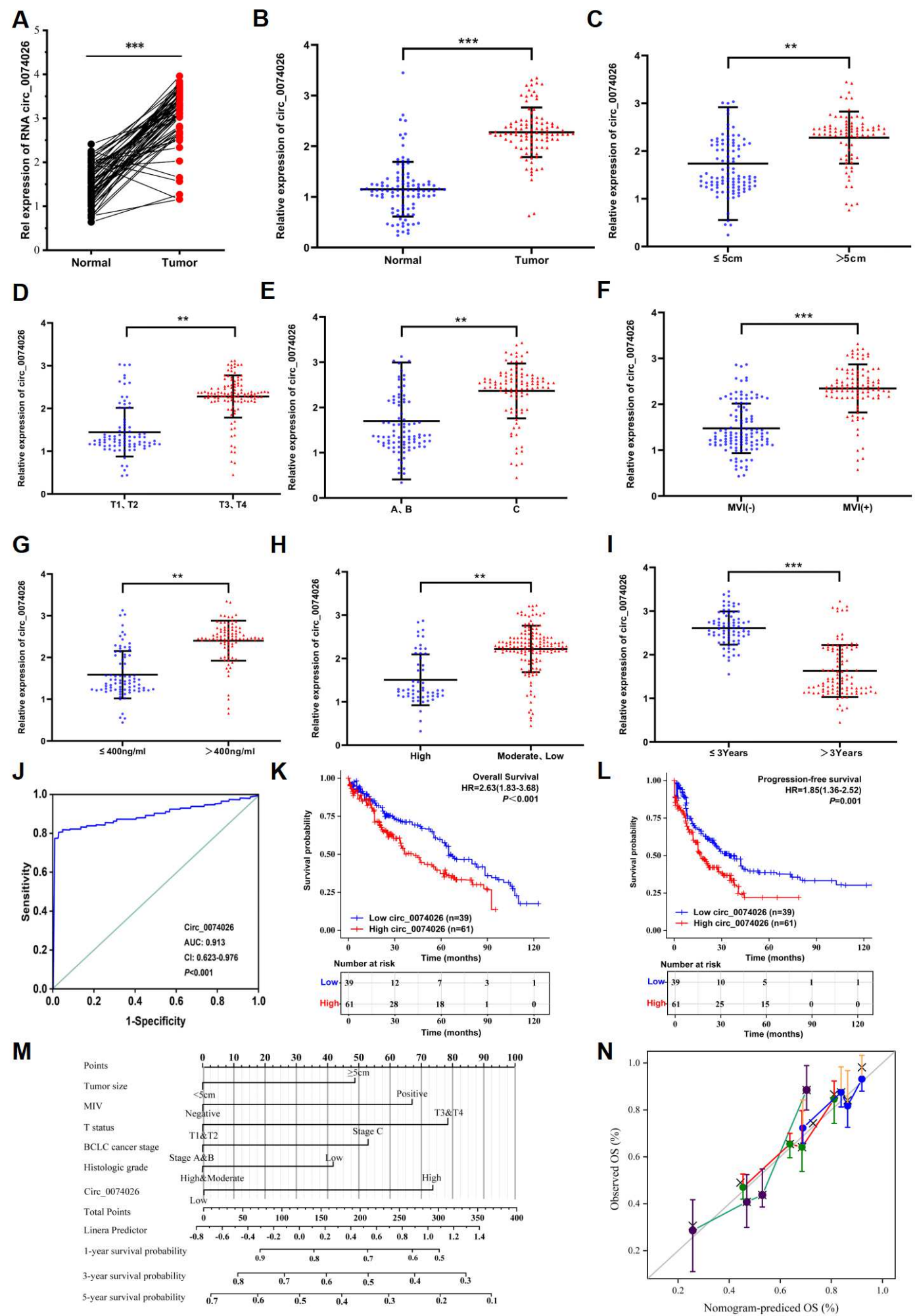
[13] Dian M J, Li J, Zhang X L, et al. MST4 negatively regulates the EMT, invasion and metastasis of HCC cells by inactivating PI3K/AKT/Snail1 axis[J]. Journal of Cancer, 2021, 12(15): 4463-4477.

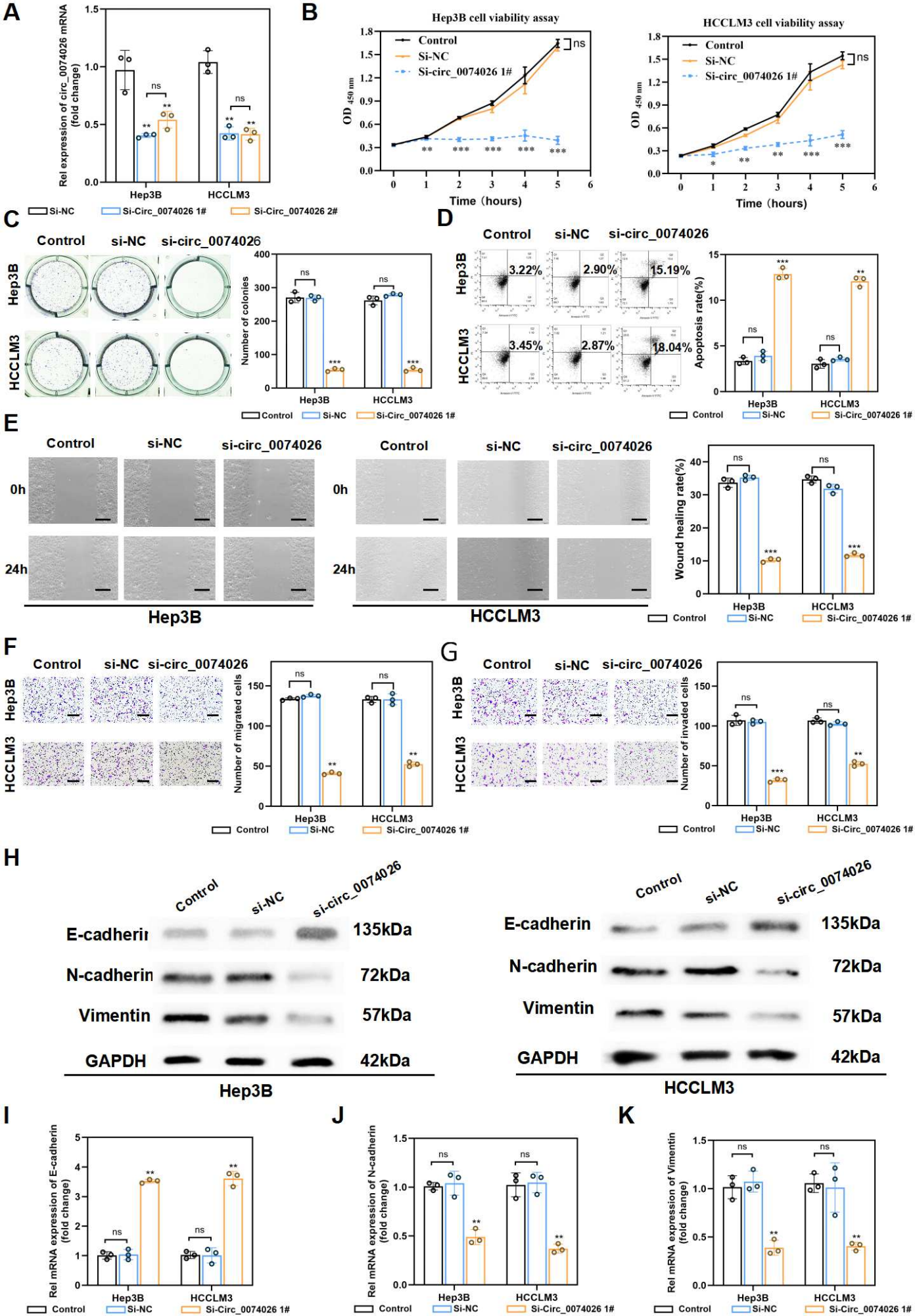
[14] Huang G, Liang M, Liu H, et al. CircRNA hsa_circRNA_104348 promotes hepatocellular carcinoma progression through modulating miR-187-3p/RTKN2 axis and activating Wnt/β-catenin pathway[J]. Cell death & disease, 2020, 11(12): 1065.

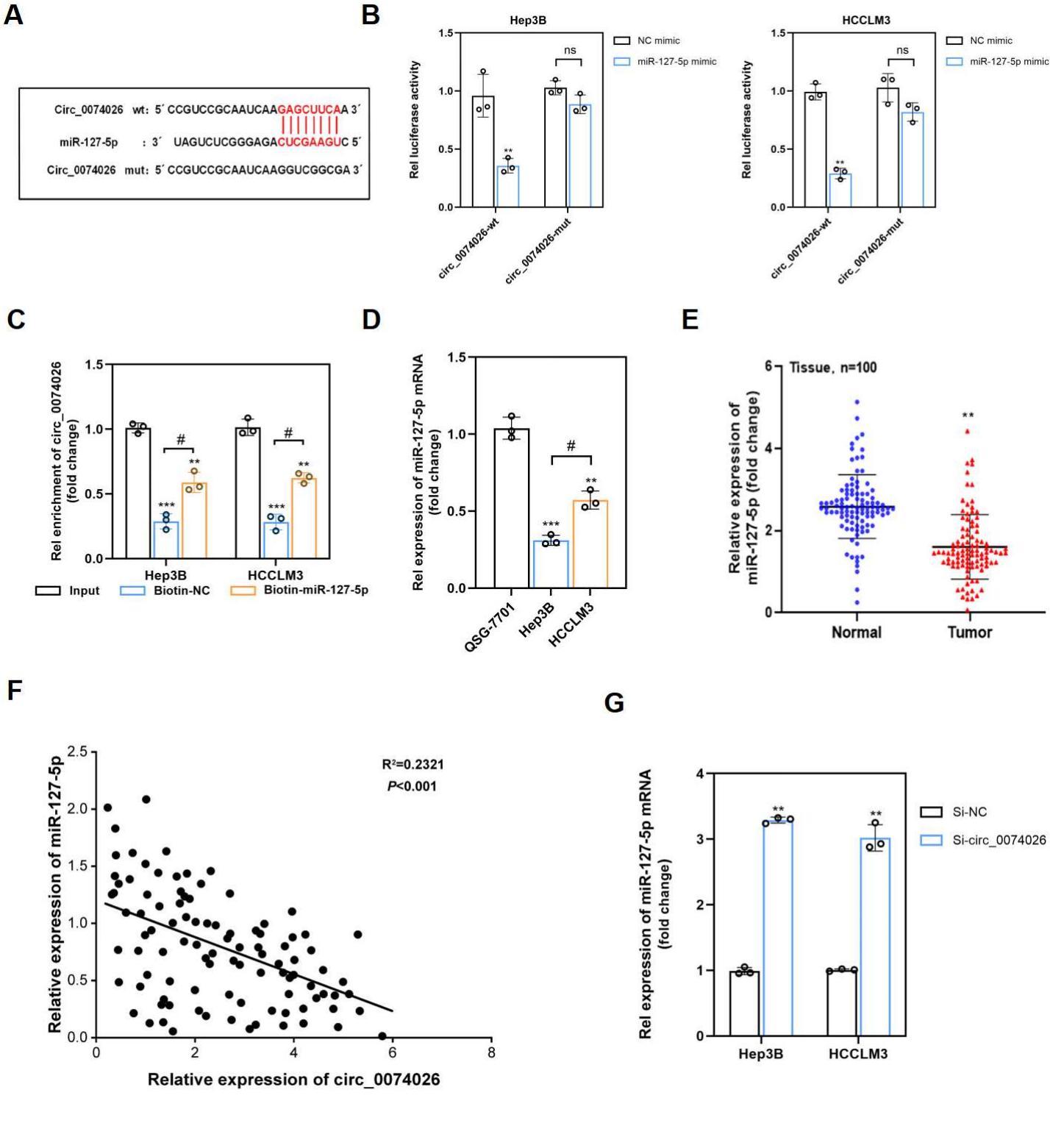
[15] Li J, Hu Z Q, Yu S Y, et al. CircRPN2 Inhibits Aerobic Glycolysis and Metastasis in Hepatocellular Carcinoma[J]. Cancer research, 2022, 82(6): 1055-1069.

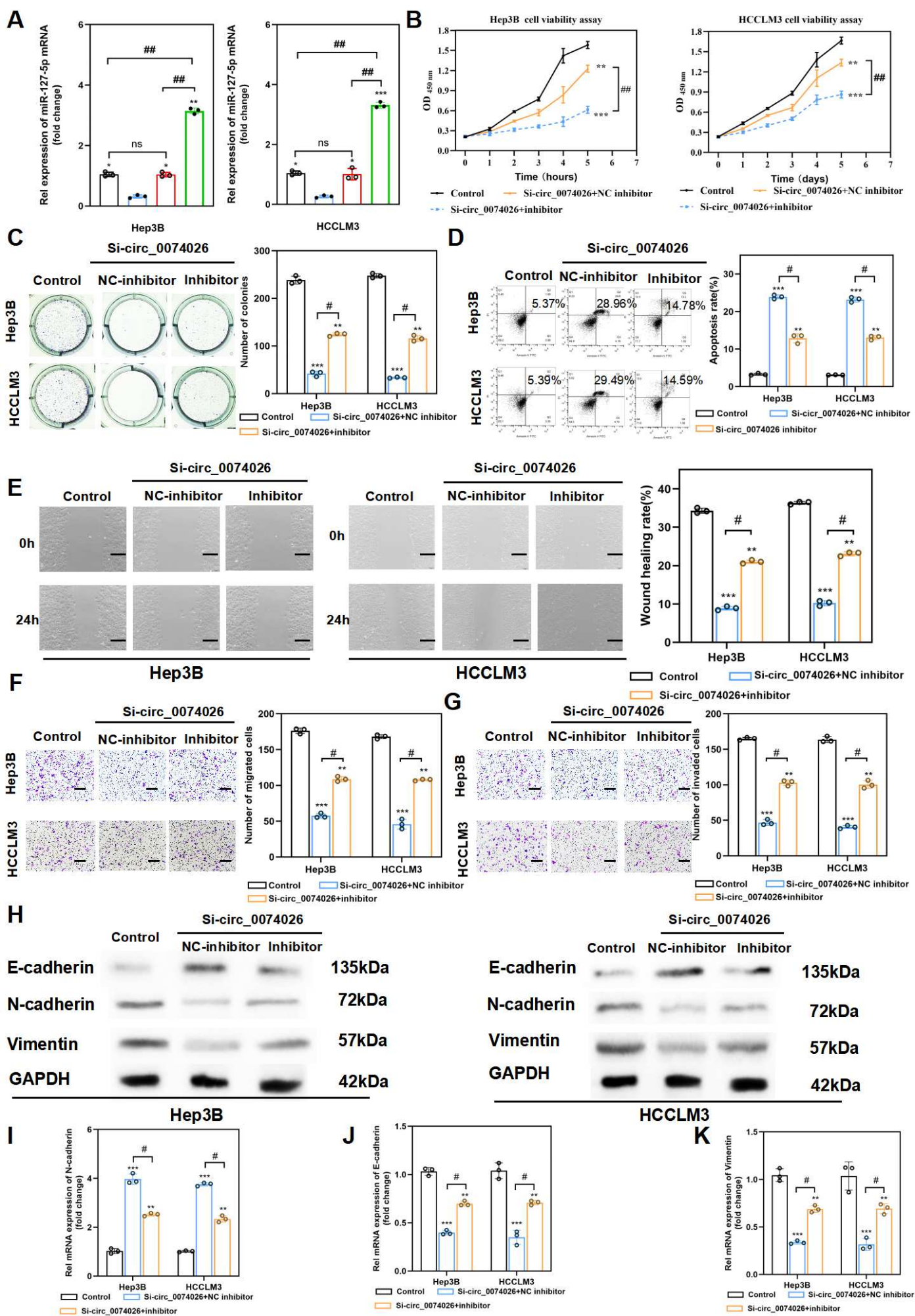
[16] Zhou Y, Mao X, Peng R, et al. CircRNAs in hepatocellular carcinoma: characteristic, functions and clinical significance[J]. Int J Med Sci, 2022, 19(14): 2033-2043.
[17] Nokkeaw A, Ariyachet C. Circular RNAs in Liver Diseases[J]. Adv Exp Med Biol, 2025, 1485: 369-394.
[18] Jabeen S, Ahmed N, Rashid F, et al. Circular RNAs in tuberculosis and lung cancer[J]. Clin Chim Acta, 2024, 561: 119810.
[19] Wang Z, Deng H, Jin Y, et al. Circular RNAs: biology and clinical significance of breast cancer[J]. RNA Biol, 2023, 20(1): 859-874.
[20] Srinivasan A, Wojciechowska M. Formation of Circular RNAs[J]. Adv Exp Med Biol, 2025, 1485: 99-115.
[21] Peng Z, Fang S, Jiang M, et al. Circular RNAs: Regulatory functions in respiratory tract cancers[J]. Clin Chim Acta, 2020, 510: 264-271.
[22] Bai K, Ma Y, Li J. Circular RNA circ_0001955 promotes hepatocellular carcinoma tumorigenesis by up-regulating alkaline ceramidase 3 expression through microRNA-655-3p[J]. Bioengineered, 2022, 13(2): 2099-2113.
[23] Li X, Lv J, Hou L, et al. Circ_0001955 Acts as a miR-646 Sponge to Promote the Proliferation, Metastasis and Angiogenesis of Hepatocellular Carcinoma[J]. Dig Dis Sci, 2022, 67(6): 2257-2268.
[24] Lin Z, Liu X, Wang H, et al. Androgen receptor promotes arachidonic acid metabolism and angiogenic microenvironment in AFP-negative hepatocellular carcinoma[J]. Nat Commun, 2025, 16(1): 6451.
[25] Liu X, Zhuang L, Yang F, et al. Clinical Outcomes of AFP-Negative Patients with Advanced HCC: A Propensity-Matched Analysis from a Retrospective Cohort Study[J]. J Hepatocell Carcinoma, 2025, 12: 1241-1252.
[26] Jeelani M. miRNAs in epilepsy: A review from molecular signatures to therapeutic intervention[J]. Int J Biol Macromol, 2024, 263(Pt 2): 130468.
[27] Hill M, Tran N. miRNA interplay: mechanisms and consequences in cancer[J]. Dis Model Mech, 2021, 14(4).
[28] Ahn J, Kim D H, Suh Y, et al. Adipose-specific expression of mouse Rbp7 gene and its developmental and metabolic changes[J]. Gene, 2018, 670: 38-45.
[29] Kim D H, Ahn J, Suh Y, et al. Retinol Binding Protein 7 Promotes Adipogenesis in vitro and Regulates Expression of Genes Involved in Retinol Metabolism[J]. Front Cell Dev Biol, 2022, 10: 876031.
[30] Zhang D M, Luo Y, Yishake D, et al. Prediagnostic dietary intakes of vitamin A and β-carotene are associated with hepatocellular-carcinoma survival[J]. Food Funct, 2020, 11(1): 759-767.
[31] Peres W A, Chaves G V, Gonçalves J C, et al. Vitamin A deficiency in patients with hepatitis C virus-related chronic liver disease[J]. Br J Nutr, 2011, 106(11): 1724-1731.
[32] Yu Y, Xu Z, Zhou H, et al. RBP7 functions as a tumor suppressor in HR + breast cancer by inhibiting the AKT/SREBP1 pathway and reducing fatty acid[J]. Cancer Cell Int, 2024, 24(1): 118.
[33] Elmasry M, Brandl L, Engel J, et al. RBP7 is a clinically prognostic biomarker and linked to tumor invasion and EMT in colon cancer[J]. J Cancer, 2019, 10(20): 4883-4891.

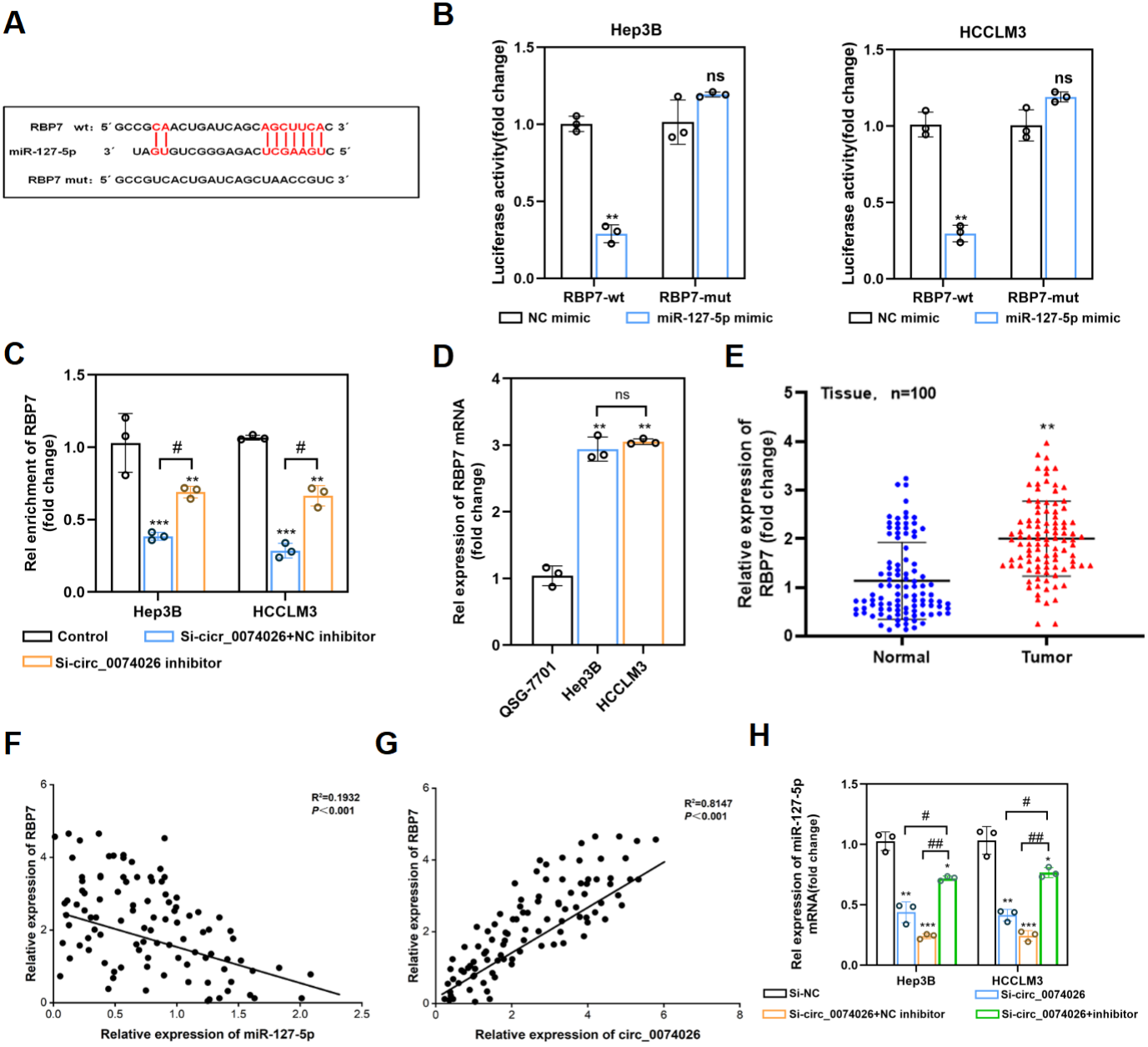

A
Z-score
Group
Tumor
Normal
T1
T2
T3
N1
N3
N2
B
GSE155367:Normal vs Tumor
Pdja < 0.05
Down
Up
-log10(P-value)
log2(Fold Change)
C
Different circRNAs KEGG
668
7
256
D
QSG-7701
Hep3B
HCCLM3
Rel expression of circRNAs (fold change)
Circ-0034211
Circ-0045628
Circ-0059722
Circ-0000387
Circ-0074311
Circ-0082731
Circ-0074026
E
Rel expression of circ_0074026 (fold change)
QSG-7701
SK
HepG2
Huh7
Hep3B
HCCLM3
F
Circ_0074026
Linear PITX1
Hep3B
Relative RNA Levels
Actinomycin D Treatment Duration (hours)
Circ_0074026
Linear PITX1
HCCLM3
Relative RNA Levels
Actinomycin D Treatment Duration (hours)
G
RNase R-
RNase R+
Hep3B
Rel RNA expression
ns
circ_0074026
Linear PITX1
RNase R-
RNase R+
HCCLM3
Rel RNA expression
ns
circ_0074026
Linear PITX1
H
DAPI
Circ_0074026
Merge
Hep3B
HCCLM3

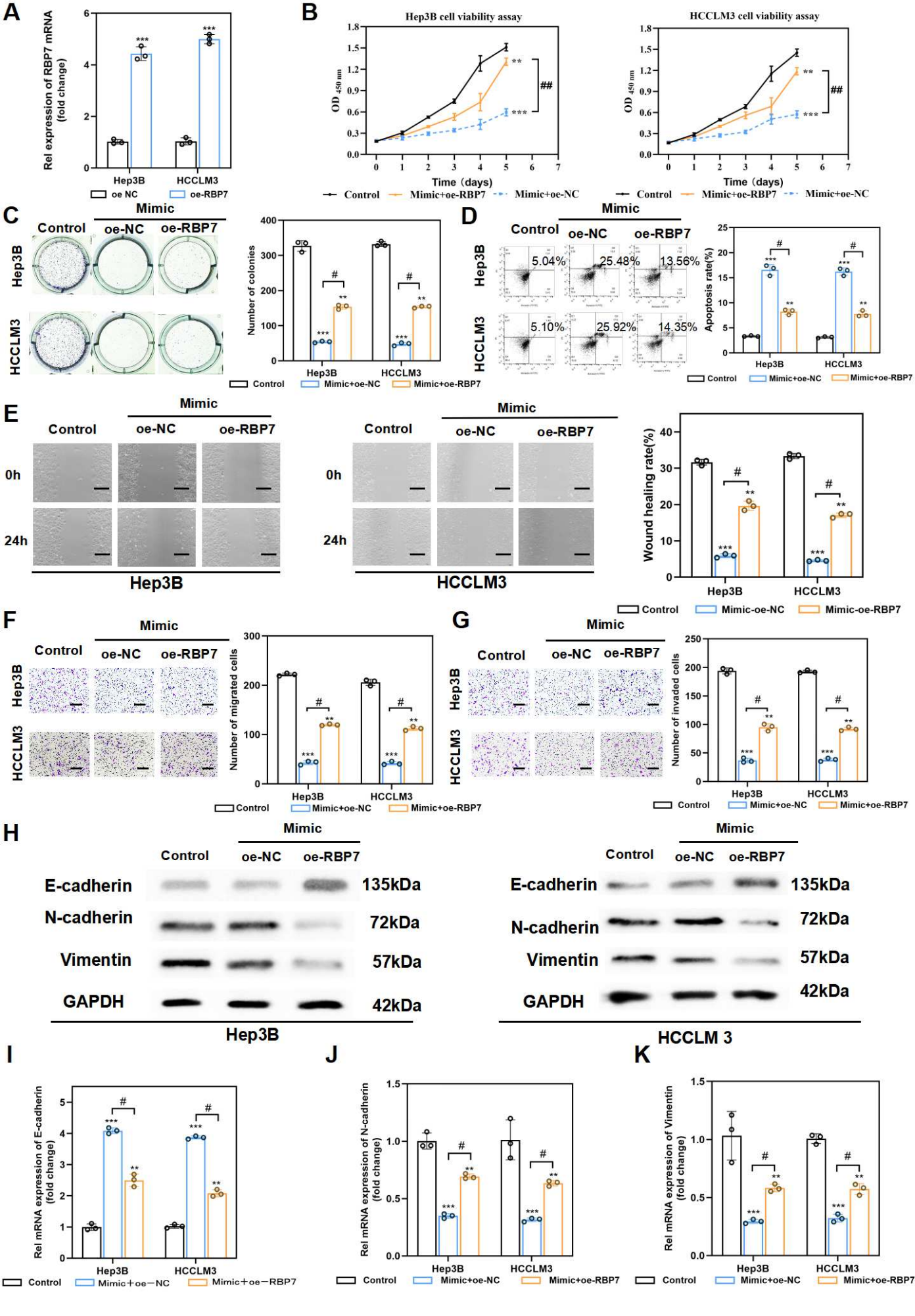

A
***
Rel expression of RNA circ_0074026
Normal
Tumor
B
***
Relative expression of circ_0074026
Normal
Tumor
C
**
Relative expression of circ_0074026
≤ 5cm
>5cm
D
**
Relative expression of circ_0074026
T1、T2
T3、T4
E
**
Relative expression of circ_0074026
A、B
C
F
***
Relative expression of circ_0074026
MVI(-)
MVI(+)
G
**
Relative expression of circ_0074026
≤ 400ng/ml
>400ng/ml
H
**
Relative expression of circ_0074026
High
Moderate、Low
I
***
Relative expression of circ_0074026
≤ 3Years
>3Years
J
Sensitivity
1-Specificity
Circ_0074026
AUC: 0.913
CI: 0.623-0.976
P<0.001
K
Overall Survival
HR=2.63(1.83-3.68)
P<0.001
Survival probability
Low circ_0074026 (n=39)
High circ_0074026 (n=61)
Time (months)
Number at risk
Low 39 12 7 3 1
High 61 28 18 1 0
L
Progression-free survival
HR=1.85(1.36-2.52)
P=0.001
Survival probability
Low circ_0074026 (n=39)
High circ_0074026 (n=61)
Time (months)
Number at risk
Low 39 10 5 1 1
High 61 25 15 0 0
M
Points
Tumor size
MIV
T status
BCLC cancer stage
Histologic grade
Circ_0074026
Total Points
Linera Predictor
1-year survival probability
3-year survival probability
5-year survival probability
≥5cm
<5cm
Positive
Negative
T3&T4
T1&T2
Stage C
Stage A&B
Low
High&Moderate
High
Low
N
Observed OS (%)
Nomogram-prediced OS (%)

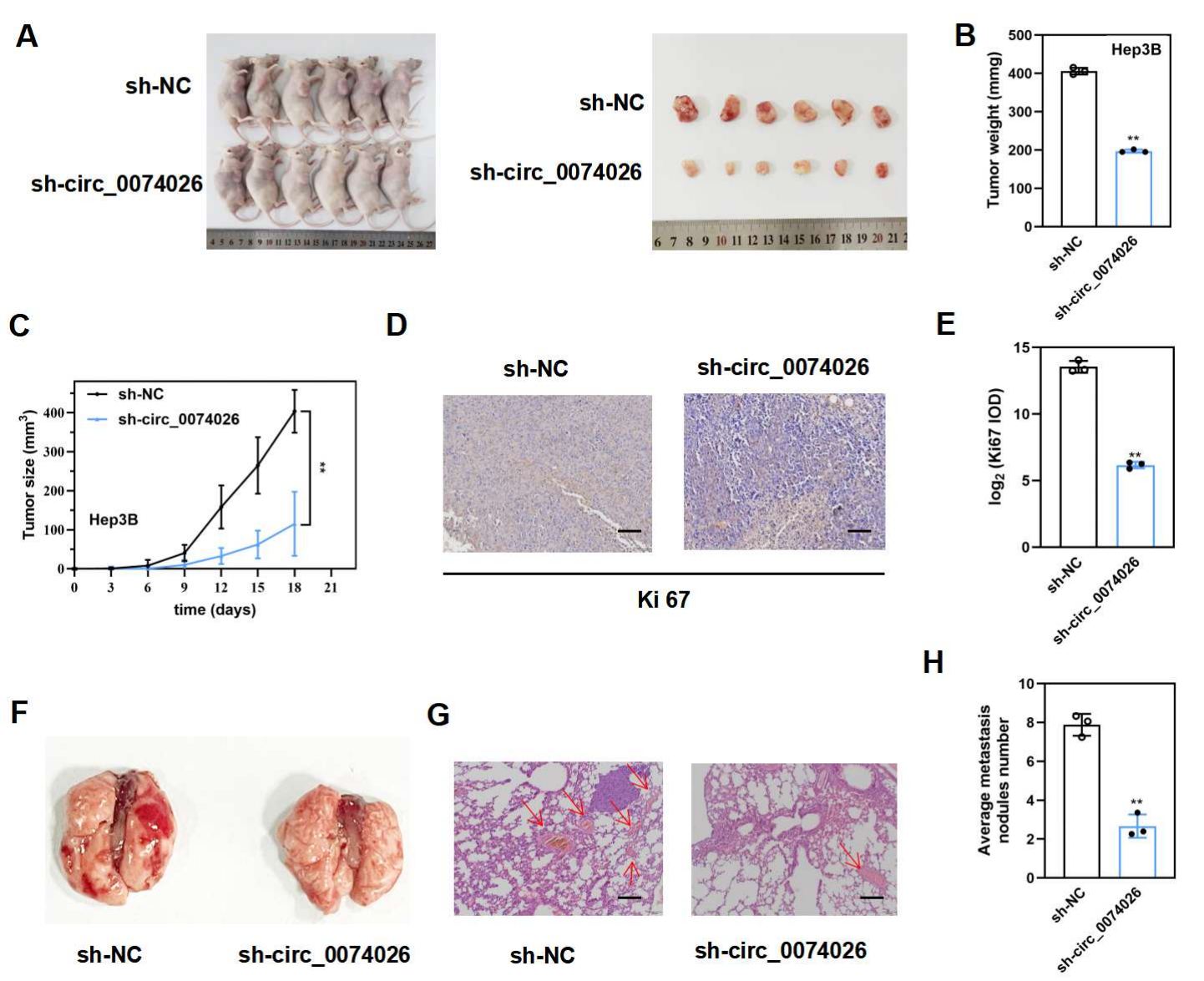

A
Rel expression of circ_0074026 mRNA (fold change)
Hep3B
HCCLM3
Si-NC
Si-Circ_0074026 1#
Si-Circ_0074026 2#
B
Hep3B cell viability assay
HCCLM3 cell viability assay
Control
Si-NC
Si-circ_0074026 1#
OD 450 nm
Time (hours)
C
Control
si-NC
si-circ_0074026
Number of colonies
D
3.22%
2.90%
15.19%
3.45%
2.87%
18.04%
Apoptosis rate(%)
E
0h
24h
Wound healing rate(%)
F
Number of migrated cells
G
Number of invaded cells
H
E-cadherin
N-cadherin
Vimentin
GAPDH
135kDa
72kDa
57kDa
42kDa
I
Rel mRNA expression of E-cadherin (fold change)
J
Rel mRNA expression of N-cadherin (fold change)
K
Rel mRNA expression of Vimentin (fold change)

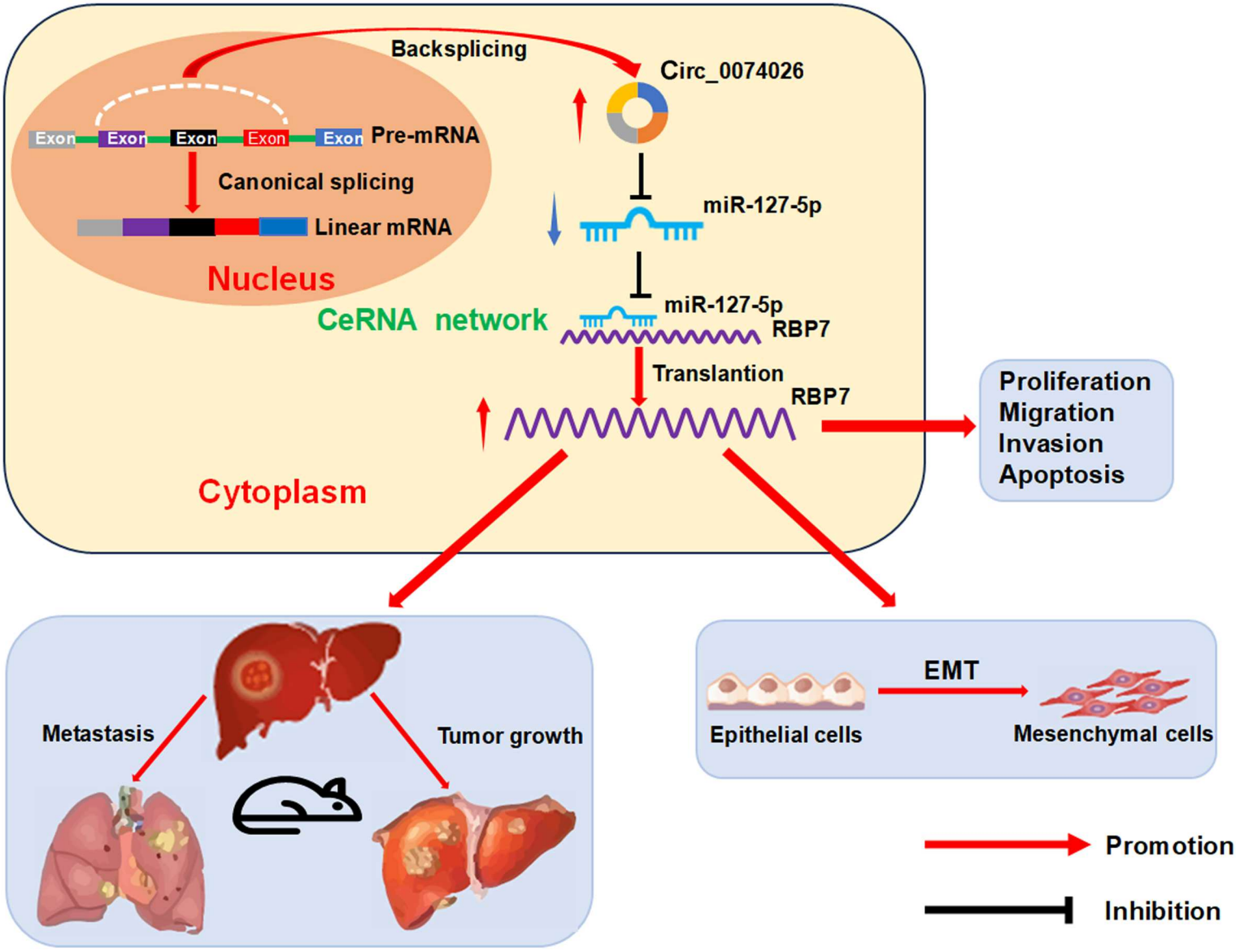

A
Circ_0074026 wt: 5′ CCGUCCGCAAUCAAGAGCUUCAA 3′
miR-127-5p : 3′ UAGUCUCGGGAGACUCGAAGUC 5′
Circ_0074026 mut: 5′ CCGUCCGCAAUCAAGGUCGGCGA 3′
B
Hep3B
HCCLM3
Rel luciferase activity
NC mimic
miR-127-5p mimic
ns
circ_0074026-wt
circ_0074026-mut
C
Rel enrichment of circ_0074026 (fold change)
Hep3B
HCCLM3
Input
Biotin-NC
Biotin-miR-127-5p
D
Rel expression of miR-127-5p mRNA (fold change)
QSG-7701
Hep3B
HCCLM3
E
Tissue, n=100
Relative expression of miR-127-5p (fold change)
Normal
Tumor
F
R²=0.2321
P<0.001
Relative expression of miR-127-5p
Relative expression of circ_0074026
G
Rel expression of miR-127-5p mRNA (fold change)
Si-NC
Si-circ_0074026
Hep3B
HCCLM3


A
Rel expression of miR-127-5p mRNA (fold change)
Hep3B
HCCLM3
B
Hep3B cell viability assay
HCCLM3 cell viability assay
OD 450 nm
Time (hours)
Time (days)
Control
Si-circ_0074026+NC inhibitor
Si-circ_0074026+inhibitor
C
Si-circ_0074026
Control
NC-inhibitor
Inhibitor
Number of colonies
D
5.37%
28.96%
14.78%
5.39%
29.49%
14.59%
Apoptosis rate(%)
Si-circ_0074026 inhibitor
E
0h
24h
Wound healing rate(%)
F
Number of migrated cells
G
Number of invaded cells
H
E-cadherin
N-cadherin
Vimentin
GAPDH
135kDa
72kDa
57kDa
42kDa
I
Rel mRNA expression of N-cadherin (fold change)
J
Rel mRNA expression of E-cadherin (fold change)
K
Rel mRNA expression of Vimentin (fold change)


A
RBP7 wt: 5′ GCCGCAACUGAUCAGCAGCUUCAC 3′
miR-127-5p 3′ UAGUGUCGGGAGACUCGAAGUC 5′
RBP7 mut: 5′ GCCGUCACUGAUCAGCUAACCGUC 3′
B
Hep3B
HCCLM3
Luciferase activity(fold change)
RBP7-wt
RBP7-mut
ns
NC mimic
miR-127-5p mimic
C
Rel enrichment of RBP7 (fold change)
Hep3B
HCCLM3
Control
Si-cicr_0074026+NC inhibitor
Si-circ_0074026 inhibitor
D
Rel expression of RBP7 mRNA (fold change)
QSG-7701
Hep3B
HCCLM3
E
Tissue, n=100
Relative expression of RBP7 (fold change)
Normal
Tumor
F
R²=0.1932
P<0.001
Relative expression of RBP7
Relative expression of miR-127-5p
G
R²=0.8147
P<0.001
Relative expression of RBP7
Relative expression of circ_0074026
H
Rel expression of miR-127-5p mRNA(fold change)
Hep3B
HCCLM3
Si-NC
Si-circ_0074026
Si-circ_0074026+NC inhibitor
Si-circ_0074026+inhibitor


A
Rel expression of RBP7 mRNA (fold change)
Hep3B
HCCLM3
oe NC
oe-RBP7
B
Hep3B cell viability assay
HCCLM3 cell viability assay
OD 450 nm
Time (days)
Control
Mimic+oe-RBP7
Mimic+oe-NC
C
Mimic
Control
oe-NC
oe-RBP7
Hep3B
HCCLM3
Number of colonies
D
5.04%
25.48%
13.56%
5.10%
25.92%
14.35%
Apoptosis rate(%)
E
0h
24h
Wound healing rate(%)
Mimic-oe-NC
Mimic-oe-RBP7
F
Number of migrated cells
G
Number of invaded cells
H
E-cadherin
N-cadherin
Vimentin
GAPDH
135kDa
72kDa
57kDa
42kDa
HCCLM 3
I
Rel mRNA expression of E-cadherin (fold change)
J
Rel mRNA expression of N-cadherin (fold change)
K
Rel mRNA expression of Vimentin (fold change)


A
sh-NC
sh-circ_0074026
sh-NC
sh-circ_0074026
B
Hep3B
Tumor weight (mmg)
500
400
300
200
100
0
**
sh-NC
sh-circ_0074026
C
sh-NC
sh-circ_0074026
Hep3B
Tumor size (mm3)
400
300
200
100
0
**
0
3
6
9
12
15
18
21
time (days)
D
sh-NC
sh-circ_0074026
Ki 67
E
log2 (Ki67 IOD)
15
10
5
0
**
sh-NC
sh-circ_0074026
H
Average metastasis nodules number
10
8
6
4
2
0
**
sh-NC
sh-circ_0074026
F
sh-NC
sh-circ_0074026
G
sh-NC
sh-circ_0074026


Backsplicing
Circ_0074026
Exon
Exon
Exon
Exon
Exon
Pre-mRNA
Canonical splicing
Linear mRNA
Nucleus
miR-127-5p
CeRNA network
miR-127-5p
RBP7
Translantion
RBP7
Proliferation
Migration
Invasion
Apoptosis
Cytoplasm
Metastasis
Tumor growth
EMT
Epithelial cells
Mesenchymal cells
Promotion
Inhibition

Supplementary Files

This is a list of supplementary files associated with this preprint. Click to download.

- Table1.docx
- Table2.docx
- Table3.docx
- Table4.docx
- SupplementaryTable.docx